Synthesis of Coordination Polymers and Discrete Complexes from the Reaction of Copper(II) Carboxylates with Pyrazole: Role of Carboxylates Basicity

Rebecca Scatena,[a,b*] Sara Massignani,[a] Arianna E. Lanza,[c] Federico Zorzi,[d] Magda Monari,[e*] Fabrizio Nestola,[d] Claudio Pettinari,[f] Luciano Pandolfo.[a*]

[a]Dipartimento di Scienze Chimiche, University of Padova, Via Marzolo, 1, I-35131 Padova, Italy.
[b]Department of Physics, Clarendon Laboratory, University of Oxford, Parks Rd., Oxford OX1 3PU, United Kingdom.
[c]Center for Nanotechnology Innovation @NEST, Istituto Italiano di Tecnologia, Piazza San Silvestro, 12, 56127 Pisa, Italy.
[d]Dipartimento di Geoscienze, University of Padova, Via Gradenigo, 6, I-35131 Padova, Italy.
[e]Dipartimento di Chimica "G. Ciamician", University of Bologna, Via Selmi, 2, I-40126 Bologna, Italy.
[f]Scuola di Farmacia, University of Camerino, Via S. Agostino, 1, I-62032 Camerino (MC), Italy.

rebecca.scaten@physics.ox.ac.uk magda.monari@unibo.it luciano.pandolfo@unipd.it

Supporting Information

EXPERIMENTAL DETAILS

Single-crystal X-ray diffraction. Instrumental details, data collection and data reduction:

a) The measurements were made at RT (297 K) on a STOE Stadi IV diffractometer equipped with a Sapphire I CCD detector by Oxford Diffraction (now Rigaku Oxford Diffraction), using graphite-monochromated Mo Kα radiation (λ = 0.71073 Å) produced with a sealed tube operating at 50 kV and 40 mA. A full sphere of reciprocal space (1380 frames) was sampled by 1° steps in ω and ϕ up ω-scan with exposure time range from 20 to 60 seconds, recording a total of 14 runs and 1245 frames. Data reduction was performed using the CrysAlis RED program.[S1] The intensities were corrected for Lorentz and polarization effects, and for absorption numerical absorption correction was obtained using X-SHAPE.[S2]

b) The X-ray intensity data were measured on a Bruker Apex II CCD diffractometer. Cell dimensions and the orientation matrix were initially determined from a least-squares refinement on reflections measured in three sets of 20 exposures, collected in three

different ω regions, and eventually refined against all data. A full sphere of reciprocal space was scanned by 0.3° ω steps. The software SMART[S3] was used for collecting frames of data, indexing reflections and determination of lattice parameters. The collected frames were then processed for integration by the SAINT program, and an empirical absorption correction was applied using SADABS.[S4]

c) Crystals of **3h** were taken out from the mother liquor into a drop of Paratone oil to avoid solvent evaporation and the selected crystal was mounted onto a glass fiber with the same oil and immediately cooled down to 173(2) K by an Oxford cryostream flow cryostat. The X-ray intensity data were measured on an Oxford Diffraction SuperNova area-detector diffractometer using mirror optics monochromated Mo Kα microsource (λ = 0.71073 Å). Data reduction was performed using the CrysalisPro[S1] program. The intensities were analytically corrected for Lorentz and polarization effects and for absorption with the Gaussian method based on the crystal shape.

Single-crystal structure solution and refinement:

d) The structure was solved by direct methods with SIR2014[S5] and refined on F^2 employing full-matrix least-squares procedures and anisotropic atomic displacement parameters for non-hydrogen atoms with SHELXL, as implemented in WinGX[S6, S7] Organic hydrogen atoms were placed in idealized positions and refined with a riding model using SHELXL.

Powder diffraction experiments:

p) **3h** was loaded in a borosilicate glass capillary (diameter 0.6 mm) which was then filled with MeOH and sealed. A PXRD pattern was collected on a Panalytical X'Pert Pro diffractometer (equipped with Cu anode, focusing mirror, capillary spinner and PixCel detector) in the range 3-70° 2θ with virtual step of 0.026° 2θ and a counting time of 500s/step. The capillary was then opened and the MeOH allowed to evaporate while PXRD patterns were measured again during one week. The patterns were fitted and indexed with HighscorePlus,[S8] and the results of Pawley fitting are reported in Table S1. The background was fitted with a Chebyshev polynomial with 15 terms and the peak profiles were fitted with a simple Caglioti function corrected for peak asymmetry.

Table S1.

Lattice parameters:	**3h** sealed	**3h'** after 1 week desolvation	restored **3h** after soaking **3h'** in MeOH
a/ Å:	10.6301(4)	9.9775(7)	10.5652(3)
b/ Å:	10.9185(4)	11.565(4)	11.0547(4)
c/ Å:	13.1287(4)	12.303(4)	13.1309(3)
alpha/ °:	86.613(4)	115.356(8)	85.758(4)
beta/ °:	74.895(3)	89.210(7)	74.864(3)
gamma/ °:	83.013(4)	94.040(4)	82.218(3)
V/ $Å^3$	1459.62	1279.55(10)	1465.60
R_{wp} %:	7.71	8.66	1.70

The diffractogram corresponding to **3h'** was used for structure solution by simulated annealing with EXPO2014[S9] in the space group *P*-1. The profile was fitted by EXPO2014 with the default procedures with minor user intervention. The unit cell was known from the previous Pawley fitting, but was also found independently by EXPO2014. The structure solution was found by following a stepwise approach. First of all, the trinuclear core $[Cu_3(\mu_3\text{-}OH)(\mu\text{-}pz)_3]^{2+}$ (Chart 1, main text) was taken from the crystal structure of **3h** and treated as a rigid body. The simulated annealing procedure was then run to determine the position and orientation of this fragment. The best partial solution was selected and 2 copies of an idealized benzoate moiety were added as independent fragments, in random positions. In addition to the coordinates and orientation for all 3 fragments, the torsion angles between the carboxylate and the phenyl groups were allowed to refine independently for both benzoate fragments, during a second set of simulated annealing runs. After convergence the best solution showed that the benzoate fragments had reached stable final positions at reasonable distances from the Cu atoms, with a final R_{wp} of 13.92 %.

The final Rietveld refinement was performed with GSAS-II[S10] on the full data range using the rigid trinuclear and semi-rigid benzoate fragments previously defined and the final refinement parameters are reported in Table 1 in the main text. The structural model so obtained does not allow to describe the internal geometry of the trinuclear core, but confirms the hypothesis of full desolvation as the cause of the transformation **3h** → **3h'**

and evidences the formation of a 1D CP thanks to the experimentally determined *syn-anti* ditopic coordination of one benzoate anion.

ADDITIONAL FIGURES

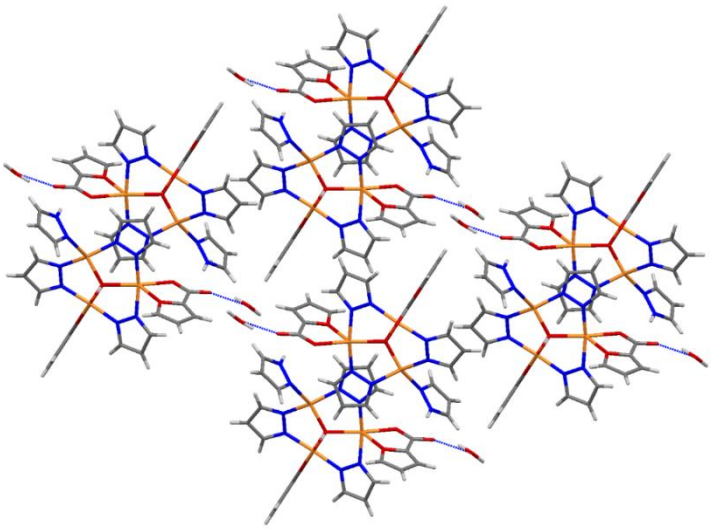

Figure S1 – View down the crystallographic *a* axis of the crystal packing of **1t**. Blue dotted lines indicate the H-bonds involving the crystallization water molecules.

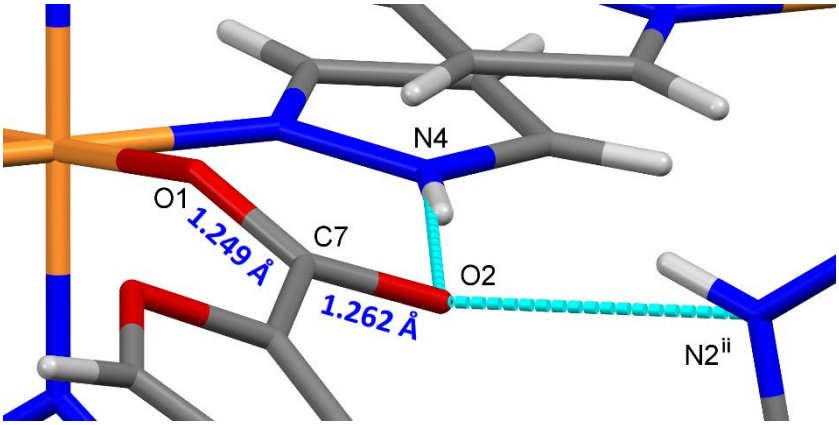

Figure S2 – H-bonds in compound **1m$_4$** (light-blue dotted lines) likely responsible of the electron delocalization in the O1-C7-O2 carboxylate moiety.

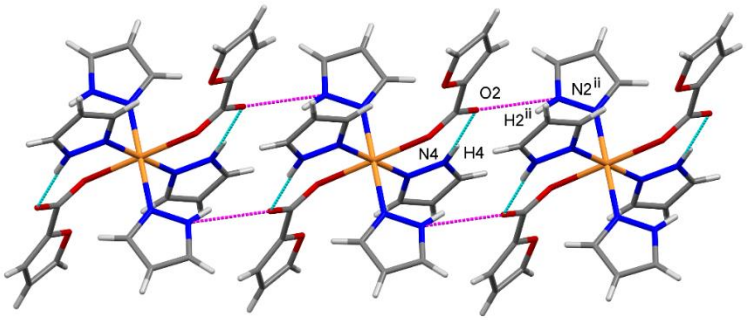

Figure S3 – 1D supramolecular assembly of **1m$_4$** based on intermolecular N2^{ii}···O2 H-bonds (magenta dashed lines). Light-blue dotted lines indicate intramolecular N4···O2 H-bonds.

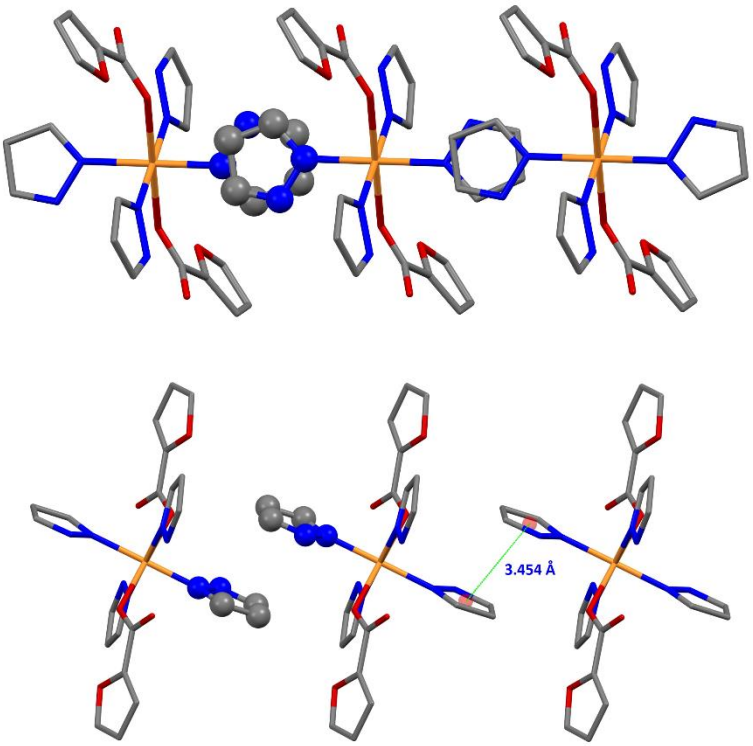

Figure S4 – 1D supramolecular assembly of **1m$_4$** based on π-π interactions. Red balls indicate the centroids of pyrazole rings. H atoms have been omitted for clarity.

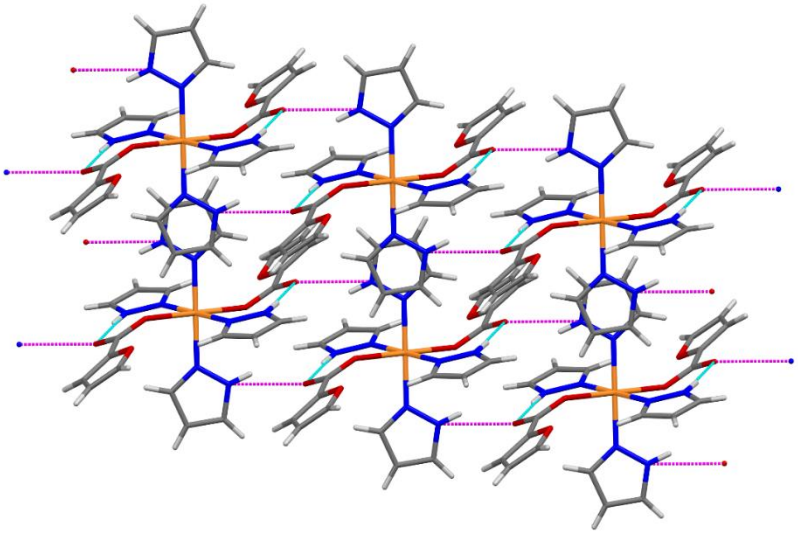

Figure S5 - 2D supramolecular assembly of **1m$_4$** generated by intermolecular H-bonds (magenta dotted lines) and π-π interactions.

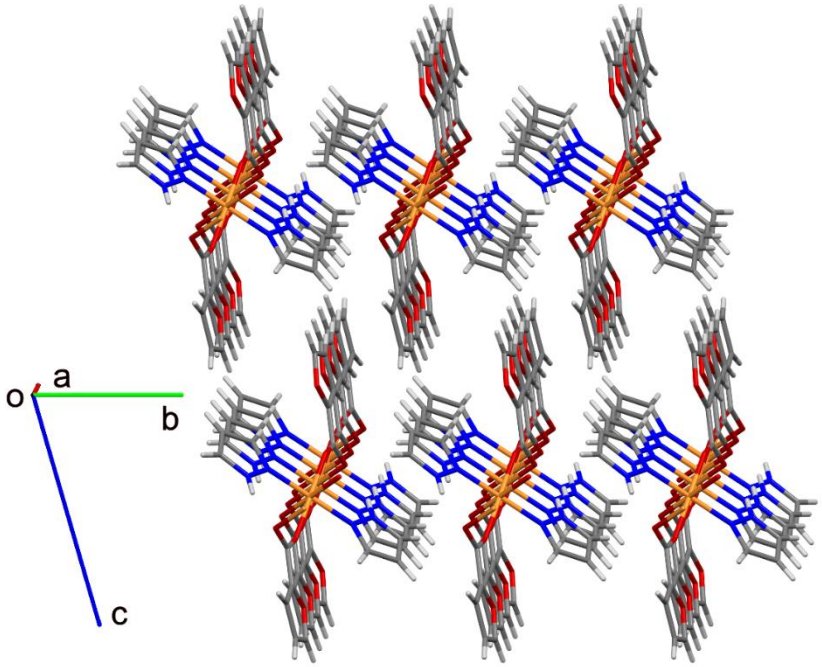

Figure S6 – Crystal packing of compound **1m$_2$**.

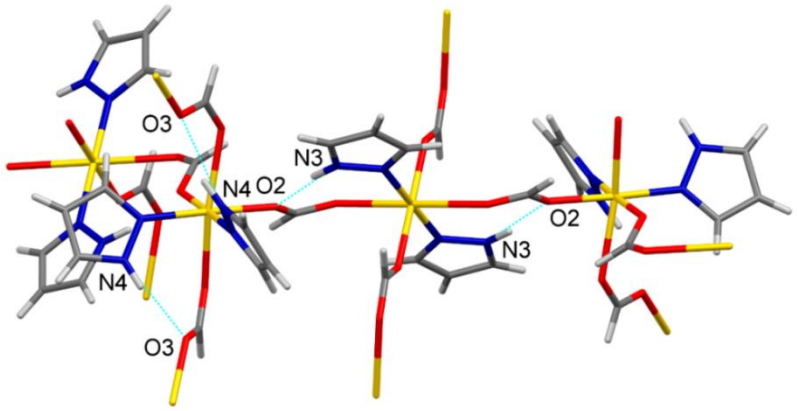

Figure S7 – H-bonds [N4···O3 2.876(2) Å, N4-H4N···O3 168(2)°; N3···O2 2.738(2) Å, N3-H3N···O2 171(2)°] (light-blue dotted lines) in compound **2d**.

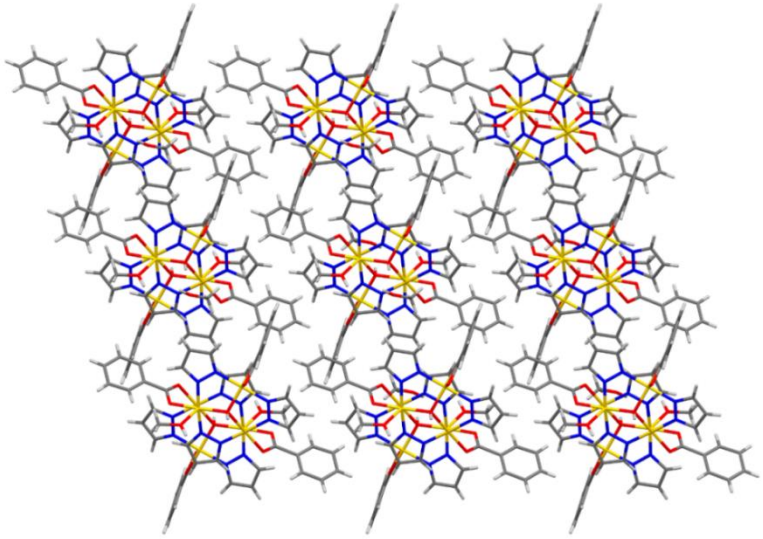

Figure S8 – View down the crystallographic *b* axis of the crystal lattice of **3h**.

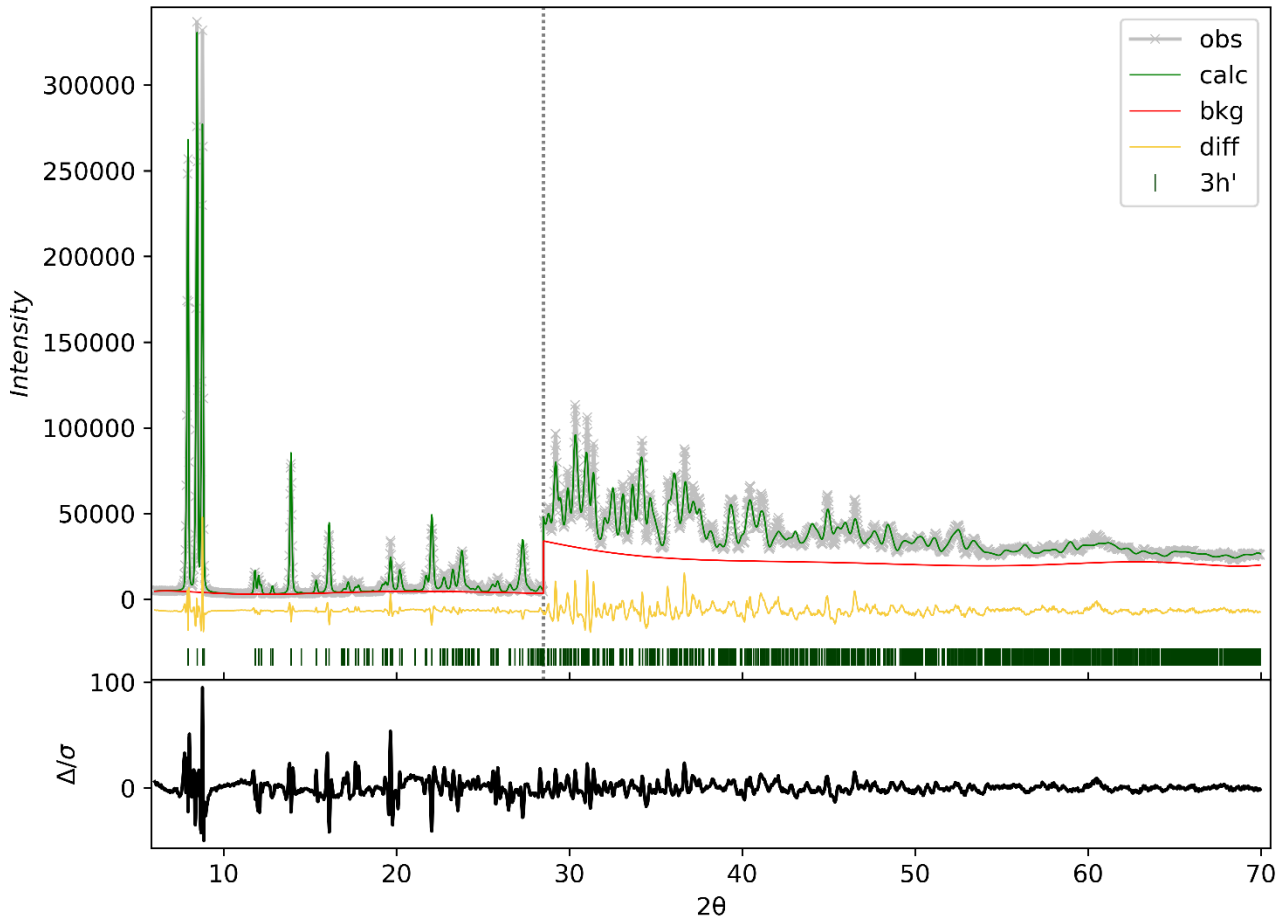

Figure S9 – Final Rietveld refinement for **3h'**. The intensities in the high angular range are ten-fold magnified.

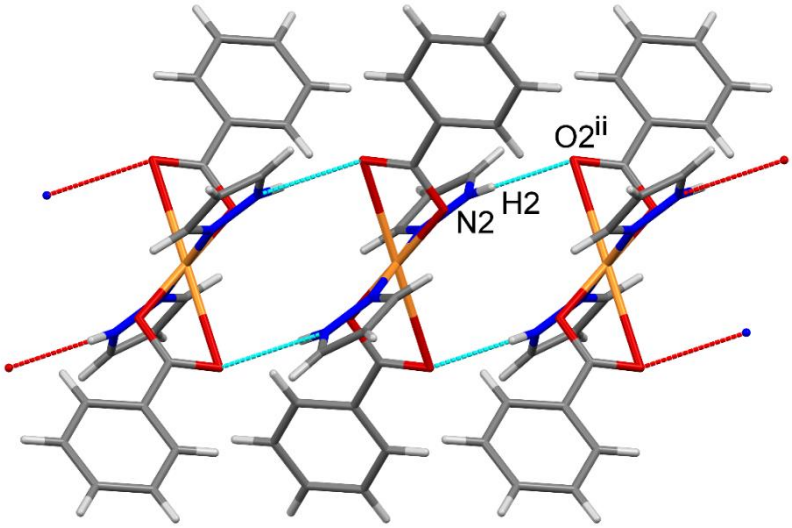

Figure S10 – View down the crystallographic *b* axis of compound **3m** evidencing H-bonds (light-blue dotted lines) generating a 1D supramolecular network.

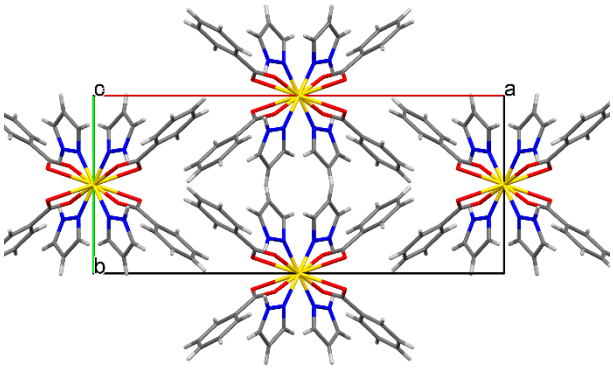

Figure S11 – View down the crystallographic *c* axis of the crystal lattice of **3m**.

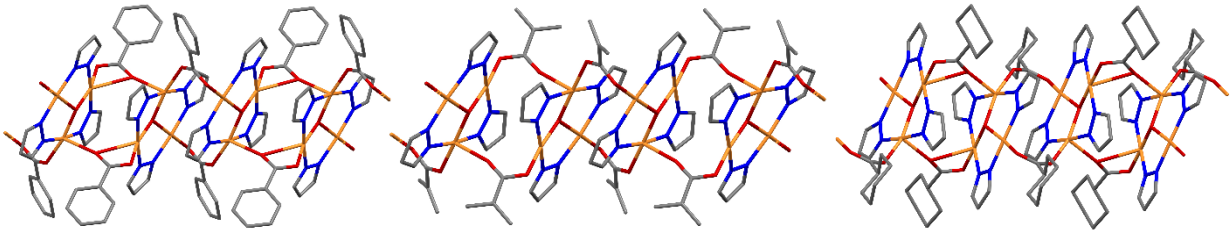

Figure S12 – Comparison among the 1D CPs structures of [{Cu_3(μ_3-OH)(μ-pz)$_3$(Benz)$_2$}$_2$], **3h'**, (left), [{Cu_3(μ_3-OH)(μ-pz)$_3$(Methacr)$_2$}$_2$] (center) and [{Cu_3(μ_3-OH)(μ-pz)$_3$(c-Hexc)$_2$}$_2$] (right).

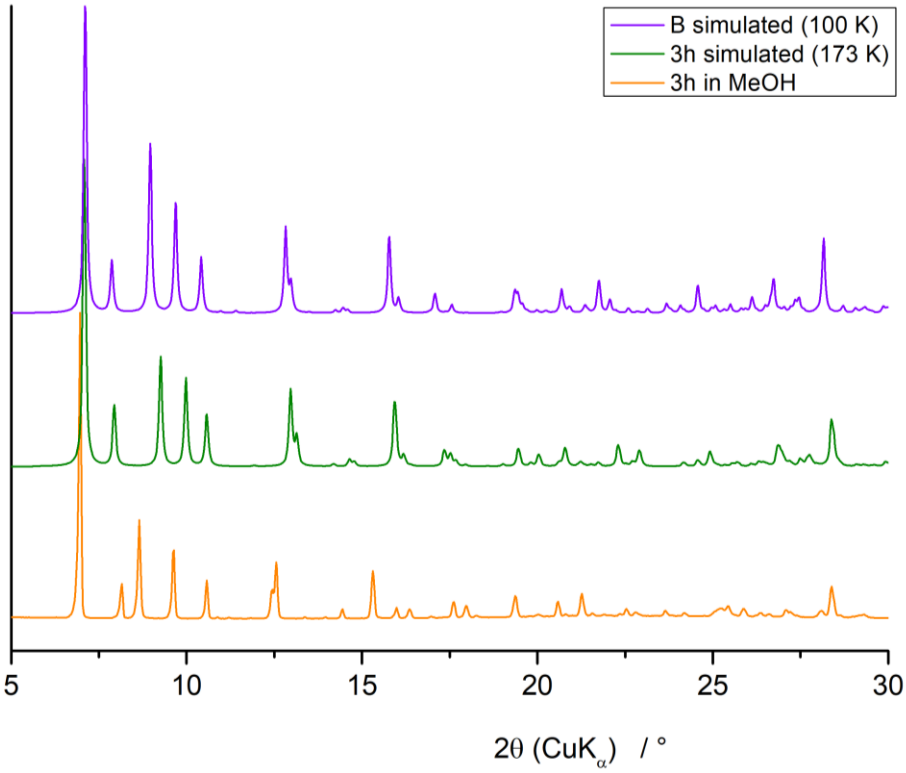

Figure S13 – The simulated PXRD pattern from the low temperature single-crystal structure of **3h** is compared with the experimental PXRD pattern of MeOH-soaked **3h** and with the pattern simulated for the analogous compound **B** (See ref. 73 of main text). The match between the simulated patterns of **3h** and **B** is excellent, while the experimental PXRD pattern at room temperature shows a slight lattice expansion and differences in the peak positions and relative intensities compared to the pattern simulated from the single-crystal structure at low temperature. It is likely that the temperature difference and the presence of excess MeOH

cause some minor difference in the crystal structure in comparison to the one determined from single crystal (see also Table S1).

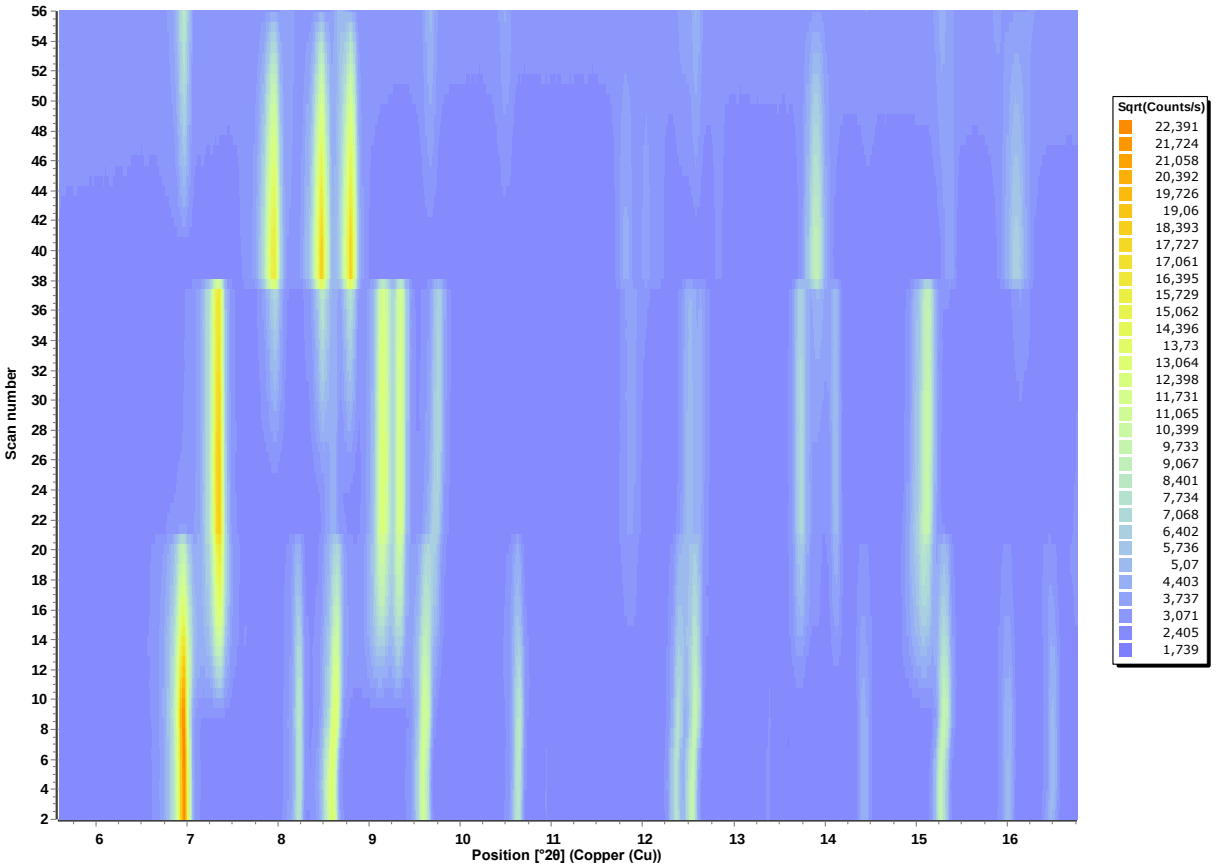

Figure S14 – Overview of the PXRD experiments. Patterns 1-7 represent pristine **3h**, patterns 8-41 are taken during the desolvation of **3h** exposed to the air, resulting in pure **3h'**. The presence of an intermediate phase, distinct from both **3h** and **3h'** is evident in the middle section of the diagram (from pattern n. 9 to pattern n. 38). Patterns 42-56 are acquired after soaking the obtained **3h'** in MeOH.

References

S1 Rigaku Oxford Diffraction, CrysalisRED and CrysalisPro Software system, various versions.

S2 X-SHAPE. Crystal Optimisation for Numerical Absorption Correction. STOE and Cie GmbH, Darmstadt, DE, **1999**.

S3 *SMART & SAINT Software Reference Manuals*, version 5.051 (Windows NT Version), Bruker Analytical X-ray Instruments Inc.: Madison, Wi, **1998**.

S4 Sheldrick, G.M. *SADABS, program for empirical absorption correction*, University of Göttingen, Germany, **1996**.

S5 Burla, M.C.; Caliandro, R.; Carrozzini, B.; Cascarano, G.L.; Cuocci, C.; Giacovazzo, C.; Mallamo, M.; Mazzone, A.; Polidori, G.; Crystal structure determination and refinement via SIR2014. *J. Appl. Crystallogr.* **2015**, 48, 306–309.

S6 Farrugia, L. J. *J. Appl. Cryst.* **1999**, 32, 837-838.

S7 Sheldrick, G. M. *Acta Cryst.* **2008**, A64, 112-122.

S8 The HighScore suite, T. Degen, M. Sadki, E. Bron, U. König, G. Nénert; Powder Diffraction / Volume 29 / Supplement S2 / December **2014**, S13-S18.

S9 Altomare, A.; Cuocci, C.; Giacovazzo, C.; Moliterni, A.; Rizzi, R.; Corriero, N.; Falcicchio, A. *J. Appl. Cryst.* **2013**, 46, 1231-1235.

S10 Toby, B.H.; Von Dreele, R.B. GSAS-II: the genesis of a modern open-source all purpose crystallography software package. *J. Appl. Crystallogr*. **2013**, 46, 544-549.